AD-A031 908 NAVAL RESEARCH LAB WASHINGTON D C F/G 20/4
SEACON II STRUMMING PREDICTIONS.(U)
OCT 76 R A SKOP, O M GRIFFIN, S E RAMBERG
UNCLASSIFIED NRL-MR-3383 NL

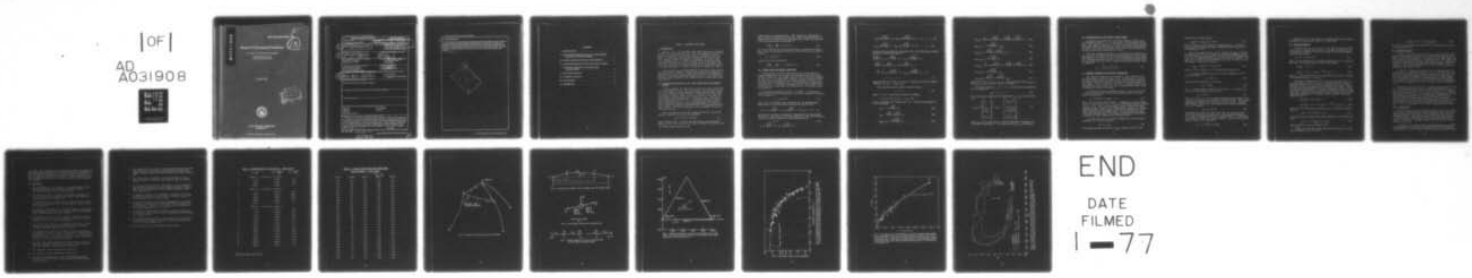

END
DATE FILMED
1-77

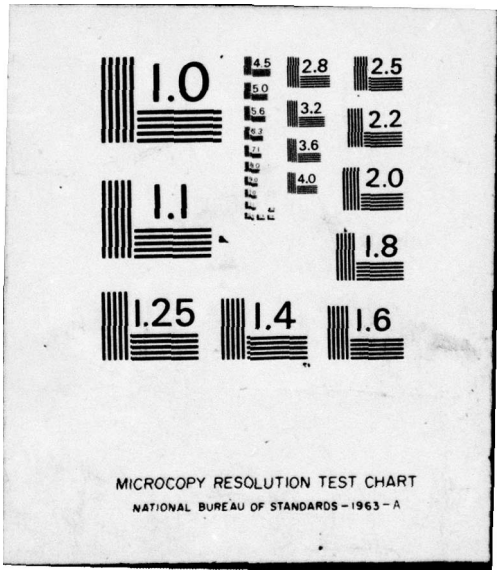
1.0
1.1
1.25
4.5
5.0
5.6
2.8
3.2
3.6
4.0
2.5
2.2
2.0
1.8
1.4
1.6
MICROCOPY RESOLUTION TEST CHART
NATIONAL BUREAU OF STANDARDS-1963-A

NRL Memorandum Report 3383

Seacon II Strumming Predictions

R. A. Skop, O. M. Griffin, S. E. Ramberg

Applied Mechanics Branch
Ocean Technology Division

October 1976

NAVAL RESEARCH LABORATORY
Washington, D.C.

SECURITY CLASSIFICATION OF THIS PAGE *(When Data Entered)*

REPORT DOCUMENTATION PAGE

READ INSTRUCTIONS BEFORE COMPLETING FORM

1. REPORT NUMBER
NRL Memorandum Report 3383

2. GOVT ACCESSION NO.

3. RECIPIENT'S CATALOG NUMBER

(9) Memorandum Rept.

4. TITLE (and Subtitle)
(6) SEACON II STRUMMING PREDICTIONS

5. TYPE OF REPORT & PERIOD COVERED
Interim report on a continuing NRL problem.

6. PERFORMING ORG. REPORT NUMBER

7. AUTHOR(s)
(10) R.A. Skop, O.M. Griffin, S.E. Ramberg

8. CONTRACT OR GRANT NUMBER(s)
(12) 22p.

9. PERFORMING ORGANIZATION NAME AND ADDRESS
Naval Research Laboratory
Washington, D.C. 20375

10. PROGRAM ELEMENT, PROJECT, TASK AREA & WORK UNIT NUMBERS
NRL Problem F02-36
Task N68305

11. CONTROLLING OFFICE NAME AND ADDRESS
Civil Engineering Laboratory
Naval Construction Battalion
Port Hueneme, California 93043

(11) 12. REPORT DATE
Oct[illegible] 1976

13. NUMBER OF PAGES
21

14. MONITORING AGENCY NAME & ADDRESS(if different from Controlling Office)
(14) NRL-MR-3383

15. SECURITY CLASS. *(of this report)*
UNCLASSIFIED

15a. DECLASSIFICATION/DOWNGRADING SCHEDULE

16. DISTRIBUTION STATEMENT *(of this Report)*

Approved for public release; distribution unlimited.

17. DISTRIBUTION STATEMENT *(of the abstract entered in Block 20, if different from Report)*

18. SUPPLEMENTARY NOTES

19. KEY WORDS *(Continue on reverse side if necessary and identify by block number)*

Moorings
Cable arrays
Seacon II
Flow-induced vibrations
Vortex shedding
Strumming

20. ABSTRACT *(Continue on reverse side if necessary and identify by block number)*

Seacon II is an ocean-based experimental mooring being used to validate or refute various array motion models. The array essentially consists of three riser cables and a subsurface horizontal delta. The cables comprising the delta are exposed to uniform currents over their lengths and hence are subject to strumming vibrations. As is known, strumming leads to a virtual increase of the drag coefficient of a cable over that value measured for a stationary cable. Since thie coefficient is a basic parameter in all array motion models, an accurate knowledge of its value is required to validate or refute the models. →next page

(Continues)

DD FORM 1 JAN 73 1473 EDITION OF 1 NOV 65 IS OBSOLETE
S/N 0102-014-6601

SECURITY CLASSIFICATION OF THIS PAGE *(When Data Entered)*

251950

20. Abstract (Continued)

In this paper, the strumming behavior of the cables comprising the Seacon II delta is examined. Employing recently-developed strumming modeling techniques, the amplitudes and frequencies of strumming are predicted. These amplitudes and frequencies are, in turn, used to predict the virtual increases of the drag coefficients of the delta cables. It is found that the values of these virtual drag coefficients are frequently 150% to 230% larger than the value of the nominal stationary drag coefficient.

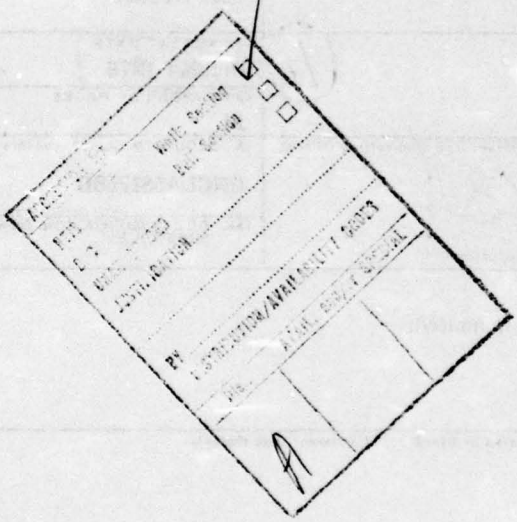

CONTENTS

SEACON II STRUMMING PREDICTIONS

I. INTRODUCTION

Seacon II (1) is an ocean based cable array being used to validate various array motion models (2,3,4). The array essentially consists of three riser cables and a horizontal delta as schematically shown in Figure 1. The cables comprising the delta see uniform currents over their lengths and hence are subject to strumming. As is well known (5,6) strumming leads to a virtual increase of the steady state drag coefficient of a cable over that value measured for a stationary cable. Since this coefficient is a basic parameter in all array motion models, an accurate knowledge of its value is required to validate the models.

In this report, the strumming behavior of the cables comprising the Seacon II delta is examined. Using recently developed strumming modeling techniques (6,7,8) the amplitudes and frequencies of strumming are predicted. These amplitudes and frequencies are, in turn, used to predict the virtual increases of the steady state drag coefficients of the delta cables.

II. EQUATIONS OF MOTION FOR A TAUT, NON-UNIFORM CABLE WITH ATTACHED MASSES

We wish to develop the equations of motion for a taut, non-uniform cable with attached masses. The situation is as illustrated in Figure 2. In this figure, s is the measure of length along the cable ranging from zero to the total length of cable L. The mass of the cable per unit length is denoted by m(s) and the displacement of the cable from its horizontal equilibrium position is given as y(s,t). The concentrated masses are given as M_1, M_2, ... and their positions along the cable represented by s_1, s_2, ... The equilibrium tension in the cable is given by T which is considered large enough to 1) hold the cable essentially straight in equilibrium and 2) be unaffected by small cable motions. The above assumptions on T are equivalent to the taut cable approximation.

Hence, the motion of each cable segment between the concentrated masses is defined by the taut string equation

$$m(s)\,\partial^2 y/\partial t^2 = T\,\partial^2 y/\partial s^2 \qquad (1)$$

where t denotes time. To obtain the conditions at the concentrated masses, we must recall that the cable has no bending rigidity and, thus,

Note: Manuscript submitted September 16, 1976.

discontinuities in slope may occur. This situation is illustrated in Figure 3 where F represents the force due to the concentrated mass. On equating the sum of the forces at the mass point to zero, one condition at the concentrated mass is obtained as

$$T\left[\frac{\partial y}{\partial s}\Big|_{+} - \frac{\partial y}{\partial s}\Big|_{-}\right] + F = 0 \tag{2}$$

The second condition at the concentrated mass is continuity of deflection. Since, by D'Alembert's Principle, the force F due to the mass is given by

$$F = -M\,\partial^2 y/\partial t^2 \tag{3a}$$

equation (2) can be rewritten as

$$T\left[\frac{\partial y}{\partial s}\Big|_{+} - \frac{\partial y}{\partial s}\Big|_{-}\right] - M\,\partial^2 y/\partial t^2 = 0 \tag{3b}$$

III. NORMAL MODES AND NATURAL FREQUENCIES

We proceed now to obtain expressions for the normal modes and natural frequencies of a taut cable with attached masses for the case in which the mass per unit length along the cable is piecewise constant. For this case, it is notationally convenient to treat each point along the cable at which the mass per unit length changes, but which is not coincident with a concentrated mass, as a point at which a concentrated mass having M = 0 is located. From equation (3b), we see that at such a point the cable slope remains continuous which is the correct transition condition.

The notation indicated in Figure 4 is adopted. To obtain the normal modes and natural frequencies of the cable, solutions to equation (1) are sought as

$$y = \psi(s)\, e^{i\omega t} \tag{4}$$

where ψ (s) is the normal mode corresponding to an eigenfrequency ω. From equation (1) and the adoped notation, $\psi(s)$ has the form

$$\psi(s) = A_i \sin\sqrt{\frac{m_i}{T}}\,\omega\, s + B_i \cos\sqrt{\frac{m_i}{T}}\,\omega\, s \quad \text{for } s_{i-1} \le s \le s_i \tag{5}$$

Applying the conditions of deflection continuity at the concentrated mass points, plus the zero deflection conditions at the cable end-points, results in relations between the coefficients given by

$$B_1 = 0 \tag{6a}$$

$$A_i \sin\sqrt{\frac{m_i}{T}}\,\omega\, s_i + B_i \cos\sqrt{\frac{m_i}{T}}\,\omega\, s_i =$$

$$A_{i+1} \sin \sqrt{\frac{m_{i+1}}{T}}\, \omega\, s_i + B_{i+1} \cos \sqrt{\frac{m_{i+1}}{T}}\, \omega\, s_i \ , \ i = 1, \ \ldots, \ I \qquad (6b)$$

$$A_{I+1} \sin \sqrt{\frac{m_{I+1}}{T}}\, \omega\, L + B_{I+1} \cos \sqrt{\frac{m_{I+1}}{T}}\, \omega\, L = 0 \qquad (6c)$$

The force balance conditions of equation (3b) yield additional relations between the coefficients given by

$$\sqrt{\frac{m_{i+1}}{T}} \left[A_{i+1} \cos \sqrt{\frac{m_{i+1}}{T}}\, \omega\, s_i - B_{i+1} \sin \sqrt{\frac{m_{i+1}}{T}}\, \omega\, s_i \right]$$

$$- \sqrt{\frac{m_i}{T}} \left[A_i \cos \sqrt{\frac{m_i}{T}}\, \omega\, s_i - B_i \sin \sqrt{\frac{m_i}{T}}\, \omega\, s_i \right]$$

$$+ \frac{M_i}{T}\, \omega \left[A_{i+1} \sin \sqrt{\frac{m_{i+1}}{T}}\, \omega\, s_i + B_{i+1} \cos \sqrt{\frac{m_{i+1}}{T}}\, \omega\, s_i \right] = 0,$$

$$i = 1, \ \ldots \ , \ I \qquad (7)$$

Equations (6b), (6c), and (7) yield 2I+1 equations for the 2I+1 coefficients A_1, A_2, B_2, $\ldots$, A_{I+1}, B_{I+1}.

These equations can be written in matrix form as

$$Q\, C = 0 \qquad (8)$$

where C is a 2I+1 column matrix having the elements

$$C = A_1, \ A_2, \ B_2, \ A_3, \ B_3, \ \ldots, \ A_{I+1}, \ B_{I+1}$$

and Q is a square matrix having rank 2I+1. The non zero elements of Q are defined by

$$Q_{1,1} = - \sin \sqrt{\frac{m_1}{T}}\, \omega\, s_1 \qquad (9a)$$

$$Q_{2,1} = - \sqrt{\frac{m_1}{T}} \cos \sqrt{\frac{m_1}{T}}\, \omega\, s_1 \qquad (9b)$$

$$Q_{2i-1,\ 2i} = \sin \sqrt{\frac{m_{i+1}}{T}}\, \omega\, s_i \qquad (9c)$$

$$Q_{2i,2i} = \frac{M_i}{T}\,\omega \sin\sqrt{\frac{m_{i+1}}{T}}\,\omega\, s_i + \sqrt{\frac{m_{i+1}}{T}}\cos\sqrt{\frac{m_{i+1}}{T}}\,\omega\, s_i \qquad (9d)$$

$$Q_{2i+1,2i} = -\sin\sqrt{\frac{m_{i+1}}{T}}\,\omega\, s_{i+1} \qquad (9e)$$

$$Q_{2i+2,2i} = -\sqrt{\frac{m_{i+1}}{T}}\cos\sqrt{\frac{m_{i+1}}{T}}\,\omega\, s_{i+1} \qquad (9f)$$

$$Q_{2i-1,2i+1} = \cos\sqrt{\frac{m_{i+1}}{T}}\,\omega\, s_i \qquad (9g)$$

$$Q_{2i,2i+1} = \frac{M_i}{T}\,\omega\cos\sqrt{\frac{m_{i+1}}{T}}\,\omega\, s_i - \sqrt{\frac{m_{i+1}}{T}}\sin\sqrt{\frac{m_{i+1}}{T}}\,\omega\, s_i \qquad (9h)$$

$$Q_{2i+1,2i+1} = -\cos\sqrt{\frac{m_{i+1}}{T}}\,\omega\, s_{i+1} \qquad (9i)$$

$$Q_{2i+2,2i+1} = \sqrt{\frac{m_{i+1}}{T}}\sin\sqrt{\frac{m_{i+1}}{T}}\,\omega\, s_{i+1} \qquad (9j)$$

In equation (9c-9j), i = 1,2 ... , I. The calculated elements $Q_{2I+2,2I}$ and $Q_{2I+2,2I+1}$ are, however, ignored in forming Q .

The eigenfrequencies ω_n, n = 1, 2, ... of the cable are determined as the solutions of

$$\det\left[\, Q\ (\omega)\,\right] = 0 \qquad (10)$$

The corresponding elements of the eigenvector $C_{i,n}\ (\omega_n)$ are then found from

$$\left[R_{J,K}(\omega_n) \right] \begin{bmatrix} C_{1,n} \\ \vdots \\ C_{K-1,n} \\ C_{K+1,n} \\ \vdots \\ C_{2I+1,n} \end{bmatrix} = -C_{K,n} \begin{bmatrix} Q_{1,K}\ (\omega_n) \\ \vdots \\ Q_{J-1,K}(\omega_n) \\ Q_{J+1,K}(\omega_n) \\ \vdots \\ Q_{2I+1,K}(\omega_n) \end{bmatrix} \qquad (11)$$

where $R_{J,K}$ is a square matrix of rank 2I obtained by eliminating the J row and K column from Q . The value chosen for $C_{K,n}$ is arbitrary.

IV. CHARACTERISTICS OF THE SEACON II DELTA CABLES

The physical characteristics of the three Seacon II delta cables are tabulated in Table 1 (9). In this table, d is the diameter of the cable. The tension in the cable is taken as the average of the maximum and minimum tensions along the cable in the no-current configuration of the array. Typically, the tensions along a cable varied less than 10% so that the taut cable approximation is valid.

Using the information in Table 1 in conjunction with equations (9), (10), and (11), the normal modes and natural frequencies, up to a maximum frequency of 25 rad/s, for each of the three Seacon II delta cables were calculated and stored on tape. Also calculated and stored on tape for each normal mode and natural frequency was the modal scaling factor I_n defined by

$$I_n = \int_0^L \psi_n^4 \, ds \Big/ \int_0^L \psi_n^2 \, ds \tag{12}$$

V. STRUMMING FREQUENCY AND AMPLITUDE CALCULATIONS

The relative orientation of the Seacon II delta, referred to an x-y base system, is shown in Figure 5 (9). In this figure, V denotes the current magnitude at the height of the delta above the bottom and θ_v denotes the current direction, referred to the x-y base system, at this height. Since, in actuality, the delta is slightly skewed to the horizontal and also possesses some sag, an average height above bottom of the delta of 2460 ft is assumed.

The naturally occurring shedding frequency ω_s from a delta cable is given by the Strouhal relation employing the normal free stream velocity component as

$$\omega_s = 2\pi S \, (V/d) \, | \sin (\theta_v - \theta) | \tag{13}$$

Here, $S = 0.21$ is the Strouhal number. In general, the cable responds in its n^{th} mode when $\omega_n \leq \omega_s \leq 1.4\,\omega_n$ with the maximum response occuring for $\omega_s \approx 1.2\,\omega_n$. For the lower modes of cable vibration this modal response is pure; however, for the higher modes of vibration, several n^{th} modes participate in the response (10) since the bandwidth for the n^{th} modal response overlaps adjacent modes. Little is known about this latter type behavior, and, in the spirit of engineering approximation, we assume pure modal responses for the Seacon cables.

To choose the mode n of the cable response for a given Strouhal frequency, ω_s, we use the equation

$$\omega_n \leq \omega_s < \omega_{n+1} \tag{14}$$

The maximum amplitude distribution $Y_{MAX}(s)$ along the cable in this

response mode is given by (6,7)

$$Y_{MAX}(s)/d = A_{MAX}\, I_n^{-\frac{1}{2}} \mid \Psi_n(s) \mid \qquad (15)$$

and the frequency of the response is approximately ω_n. In equation (15), A_{MAX} is a dimensionless modal response amplitude and I_n is defined by equation (12).

As has been shown in refs. (6,7,8), the value of A_{MAX} is uniquely determined by the value of a response or stability parameter S_G which is itself related to certain physical properties of the strumming structure. The relationship between A_{MAX} and S_G is shown in Figure 6. The legend for the data points can be found in ref (7). The solid line in this figure is given by the formula

$$A_{MAX} = 1.29 \Big/ (1 + 0.43\, S_G)^{3.35} \qquad (16)$$

which is a least squares fit to the experimental data points.

The response parameter S_G for a structure strumming in its n^{th} mode is defined by

$$S_G = 2\pi S^2\, k_s \qquad (17a)$$

where the reduced damping k_s is given by

$$k_s = \pi c/2\rho\nu\beta_n \qquad (17b)$$

Here, ν is the kinematic viscosity of the fluid, ρ is its density, β_n is the vibratory Reynolds number given by

$$\beta_n = \omega_n d^2/4\nu \qquad (18)$$

and c (lb s/ft^2) is the viscous damping constant per unit length of the structure at frequency ω_n as measured in the still fluid. This damping constant thus includes both structural and fluid effects. Recently, Skop, Ramberg, and Ferer (11) have shown that the fluid contribution to c, c_f, is given by

$$c_f = 4.5\, \pi\rho\nu\, \beta_n^{\frac{1}{2}} \qquad (19)$$

and Ramberg and Griffin (12) have found that, for the Seacon type cables, the structural contributions to c are negligible compared to c_f. Substituting equation (19) into equation (17b), k_s for the Seacon delta cables is found to be uniquely defined in terms of the vibratory Reynolds number of the response as

$$k_s = 4.5\, \pi^2/2\beta_n^{\frac{1}{2}} = 22.2/\beta_n^{\frac{1}{2}} \qquad (20)$$

Equations (13) to (20) define the strumming frequency and response amplitude of the Seacon delta cables to a flow field.

VI. DRAG AMPLIFICATION

In Figure 7 (5, 13, 14, 15, 16, 17), the ratio of the drag coefficient C_D on a strumming rigid cylinder to the drag coefficient C_{DO} on the stationary cylinder is plotted as a function of the wake response parameter w_r defined by

$$w_r = (1 + 2Y/d)\ (\omega/\omega_s) \tag{21}$$

Here, Y is the amplitude of the cylinder vibration and ω its frequency. The solid line in this figure is given by the formula

$$C_D/C_{DO} = 1.0,\ w_r < 1 \tag{22a}$$

$$C_D/C_{DO} = 1.0 + 1.16\ (w_r - 1)^{0.65},\ w_r \geq 1 \tag{22b}$$

which is a least squares fit to the experimental data points including the constraint $C_D/C_{DO} = 1$ when $w_r = 1$.

Experiments by Ramberg and Griffin (14, 18) have shown that the near wake pattern behind a point on a strumming flexible cylinder is basically identical to the near wake pattern behind a rigid cylinder strumming with the same amplitude and frequency as the point. That is, the near wake pattern behind a point on a strumming flexible cylinder is essentially independent of the spanwise variation in amplitude about that point. Using this information, it can be surmised that the local drag coefficient $C_D(s)$ on a strumming flexible cylinder is given by equations (22) as

$$C_D(s)/C_{DO} = 1.0,\ w_r(s) < 1 \tag{23a}$$

$$C_D(s)/C_{DO} = 1.0 + 1.16\ [w_r(s) - 1]^{0.65},\ w_r(s) \geq 1 \tag{23b}$$

where the local wake response parameter $w_r(s)$ is defined by equation (21) as

$$w_r(s) = [1 + 2Y(s)/d]\ (\omega/\omega_s) \tag{24}$$

In particular, for a Seacon delta cable strumming in its n^{th} mode, we have

$$w_r(s) = [1 + 2Y_{MAX}(s)/d]\ (\omega_n/\omega_s) \tag{25}$$

where $Y_{MAX}(s)/d$ is given by equation (15).

Finally, we obtain the virtual drag coefficient C_{DV} for a delta cable strumming in its n^{th} mode as

$$C_{DV}/C_{DO} = (1/L) \int_0^L [C_D(s)/C_{DO}]\, ds \qquad (26)$$

It is this virtual steady state drag coefficient which should be used in array motion models.

VII. NUMERICAL RESULTS

In Table 2, the calculated values of C_{DV}/C_{DO} for each of the three Seacon II delta cables are listed for various current magnitudes and angles supplied by Albertsen (9). The value of the virtual steady drag coefficient C_{DV} due to strumming is frequently 150% to 230% larger than the value of the nominal stationary drag coefficient C_{DO}. These large increases in the steady drag coefficient would be expected to have a significant effect on the magnitude of the array motions predicted by the array motion models (2,3,4).

In Figure 8, supplied by Albertsen (19), the measured motions of a point near the intersection of cables 1 and 3 on the delta are compared to the predicted motions during a semi-diurnal tidal cycle. The predicted motions were obtained using the Fortran IV program DESADE (2). The magnitude and direction (predominantly from the southeast) of the current during the cycle can be inferred from the displacement of the point of measurement from its no current location designated by "X".

The measured motion of the point is shown in Figure 8 by the solid line. The predicted motion using a constant drag coefficient $C_D = C_{DO} = 1.55$ is given by the dashed line with circles (--0--). Finally, the predicted motion using $C_D = (C_{DV}/C_{DO})\, C_{DO}$, with C_{DV}/C_{DO} calculated from equation (26) and $C_{DO} = 1.55$, is shown by the dashed line (-----). Excellent agreement between the predicted and measured motions is obtained when the virtual steady drag coefficients are employed. It is also apparent, for the larger current magnitudes, that the displacements predicted using the nominal stationary drag coefficient ($C_D = C_{DO} = 1.55$) are considerably smaller than the measured displacements.

VIII. CONCLUSIONS

The most recent cable-strum modeling techniques have been used to calculate the vibration-induced virtual increases in the steady state drag coefficients of the Seacon II delta cables over their nominal stationary values. These amplified drag coefficients have been used in the array motion model DESADE (2) to predict the motions of the Seacon II cable array. Agreement between the predicted and measured motions is excellent.

The results of this work clearly show the importance of considering strumming and its resultant drag amplification in the design of mooring arrays. It must be noted, however, that much research remains

to be done. At the present time, the techniques used in this paper for calculating drag amplification are limited to cables in a uniform flow. Thus, for example, nothing can yet be said with accuracy about any possible drag amplification for the Seacon II anchor legs which, along their lengths, are influenced by currents that vary both in magnitude and direction.

IX. REFERENCES

1. T.R. Kretschmer, et. al., "Seacon II: An Instrumented Tri-Moor for Evaluating Cable Structure Design Methods," Offshore Technology Conference Paper OTC 2365, May 1975.

2. R.A. Skop and J. Mark, "A Fortran IV Program for Computing the Static Deflections of Structural Cable Arrays," Naval Research Laboratory Report 7640, August 1973.

3. R.F. Dominguez and C.E. Smith, "Dynamic Analysis of Cable Systems," Journal of the Structural Division, ASCE, 98, No. ST8, pp. 1817-1834, August 1972.

4. R.L. Webster, "Nonlinear Static and Dynamic Response of Underwater Cable Structures Using the Finite Element Method," Offshore Technology Conference Paper OTC 2322, May 1975.

5. O.M. Griffin, R.A. Skop, and G.H. Koopmann, "The Vortex-Excited Resonant Vibrations of Circular Cylinders," Journal of Sound and Vibration, 31, 2, pp. 235-249, November 1973.

6. O.M. Griffin, R.A. Skop, and S.E. Ramberg, "The Resonant, Vortex-Excited Vibrations of Structures and Cable Systems," Offshore Technology Conference Paper OTC 2319, May 1975.

7. R.A. Skop and O.M. Griffin, "On a Theory for the Vortex-Excited Oscillations of Flexible Cylindrical Structures," Journal of Sound and Vibration, 41, 3, pp. 263-274, August 1975; also "The Vortex-Induced Oscillations of Structure," letter to Journal of Sound and Vibration, 44, 2, pp. 303-305, January 1976.

8. W.D. Iwan, "The Vortex Induced Oscillation of Elastic Structural Elements," Journal of Engineering for Industry, ASME, to appear 1976; also available as ASME Paper No. 75-DET-28.

9. N.D. Albertsen, private communication, March 1976.

10. J.K. Vandiver, private communication, March 1976.

11. R.A. Skop, S.E. Ramberg, K.M. Ferer, "Added Mass and Damping Forces on Circular Cylinders," Naval Research Laboratory Report 7970, March 1976.

12. S.E. Ramberg and O.M. Griffin, "Some Transverse Resonant Vibration Characteristics of Wire Rope with Application to Flow-Induced Cable Vibrations," Naval Research Laboratory Report 7821, December 1974.

13. O.M. Griffin and S.E. Ramberg, "On Vortex Strength and Drag in Bluff Body Wakes," Journal of Fluid Mechanics, 69, pp. 721-728, 1975.

14. S.E. Ramberg and O.M. Griffin, "The Effects of Vortex Coherence, Spacing, and Circulation on the Flow-Induced Forces on Vibrating Cables and Bluff Structures," Naval Research Laboratory Report 7945, January 1976.

15. Y. Tanida, A. Okajima, and Y. Watanabe, "Stability of a Circular Cylinder Oscillating in Uniform Flow or in a Wake," Journal of Fluid Mechanics, 61, pp. 769-784, 1973.

16. G. Diana and M. Falco, "On the Forces Transmitted to a Vibrating Cylinder by a Blowing Fluid (Experimental Study and Analysis of the Phenomenon)," Mecchanica (J. Italian Assoc. for Theoretical and Applied Mechanics) 6, pp. 9-22, 1971.

17. D.W. Meyers, "Transverse Oscillations of a Circular Cylinder in Uniform Flow," Masters Thesis, Naval Postgraduate School, Monterey, CA., December 1975.

18. S.E. Ramberg and O.M. Griffin, "Vortex Formation in the Wake of a Vibrating, Flexible Cable," Journal of Fluids Engineering, ASME, 96, pp. 317-322, December 1974.

19. N.D. Albertsen, private communication, August 1976.

TABLE 1. CHARACTERISTICS OF THE SEACON II DELTA CABLES

i	s_i (ft)	m_i^* $\left(\frac{\text{lb s}^2}{\text{ft}^2}\right)$	M_i^* $\left(\frac{\text{lb s}^2}{\text{ft}}\right)$
	Cable 1, T = 611 lb, d = 0.712 in.		
1	1.5	0.0215	3.56
2	999.5	0.0215	2.33
3	1001.0	0.0215	----
	Cable 2, T = 662 lb, d = 0.715 in.		
1	1.5	0.0216	3.56
2	333.0	0.0216	10.81
3	666.0	0.0216	10.83
4	999.5	0.0216	3.56
5	1001.0	0.0216	----
	Cable 3, T = 701 lb, d = 0.625 in.		
1	1.5	0.0243	2.33
2	76.5	0.0243	1.28
3	78.0	0.0243	0.00
4	81.5	0.0152	2.00
5	381.0	0.0152	1.44
6	556.0	0.0152	3.47
7	681.0	0.0152	1.44
8	776.0	0.0152	3.34
9	856.0	0.0152	1.38
10	921.0	0.0152	2.28
11	923.0	0.0152	0.00
12	924.5	0.0211	1.28
13	999.5	0.0211	2.33
14	1001.0	0.0211	----

*Mass plus added mass of water.

TABLE 2. VIRTUAL STEADY STATE DRAG COEFFICIENTS FOR THE SEACON II DELTA CABLES

V(ft/s)	θ_v(deg)	C_{DV} / C_{DO} Cable 1	Cable 2	Cable 3
.180	162	1.74	1.78	1.64
.176	159	1.57	1.80	1.77
.164	154	2.06	1.89	1.72
.176	142	1.93	1.80	1.61
.185	152	1.77	1.71	1.62
.184	143	1.90	1.73	1.93
.190	141	1.80	1.68	1.53
.200	134	2.20	1.65	1.61
.248	120	2.28	1.51	1.00
.221	115	2.18	1.73	1.49
.261	123	2.25	1.96	1.00
.277	141	2.16	1.71	1.63
.233	102	2.18	1.89	1.96
.240	102	2.14	1.91	1.96
.315	98	2.33	1.64	1.58
.297	96	2.27	1.79	1.55
.335	84	2.35	1.27	1.69
.320	84	2.29	1.32	1.50
.303	78	2.26	1.70	1.66
.289	76	2.20	1.77	1.68
.317	68	2.28	1.18	1.31
.335	70	2.31	1.00	1.27
.303	62	2.28	1.00	1.26
.287	51	2.22	1.22	1.63
.244	58	2.14	1.00	1.58
.226	41	2.15	1.00	1.56
.185	18	1.74	1.36	1.58
.151	31	1.92	1.00	1.28
.135	117	2.17	1.48	1.00

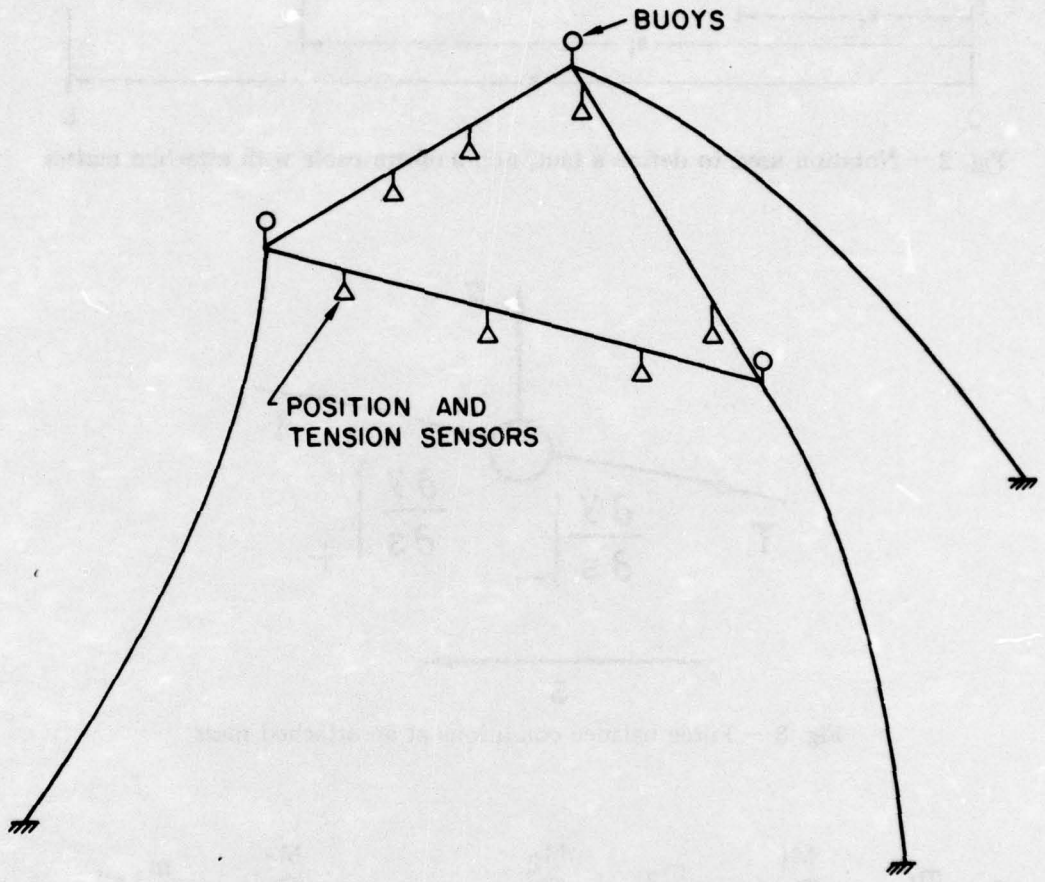

Fig. 1 — Schematic drawing of the Seacon II cable array

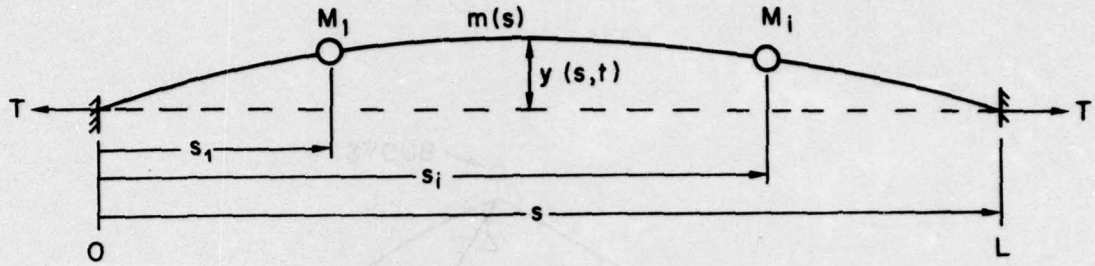

Fig. 2 — Notation used to define a taut, non-uniform cable with attached masses

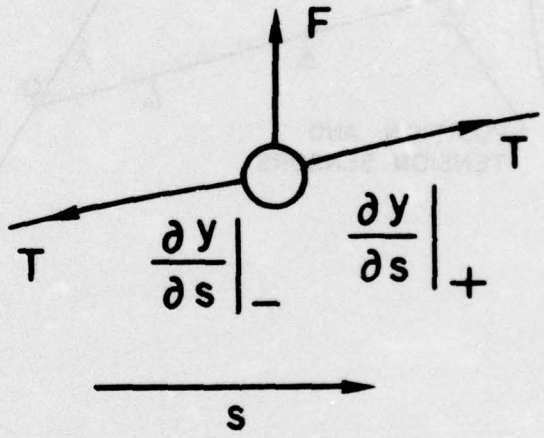

Fig. 3 — Force balance conditions at an attached mass

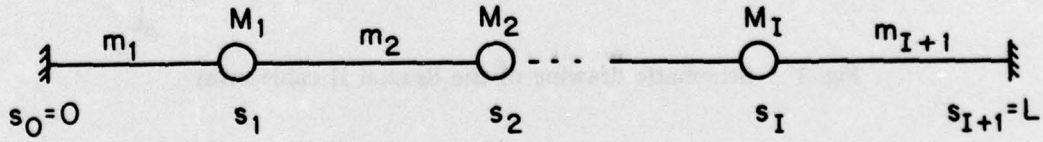

Fig. 4 — Notation adopted for the case in which the mass per unit length is piecewise constant

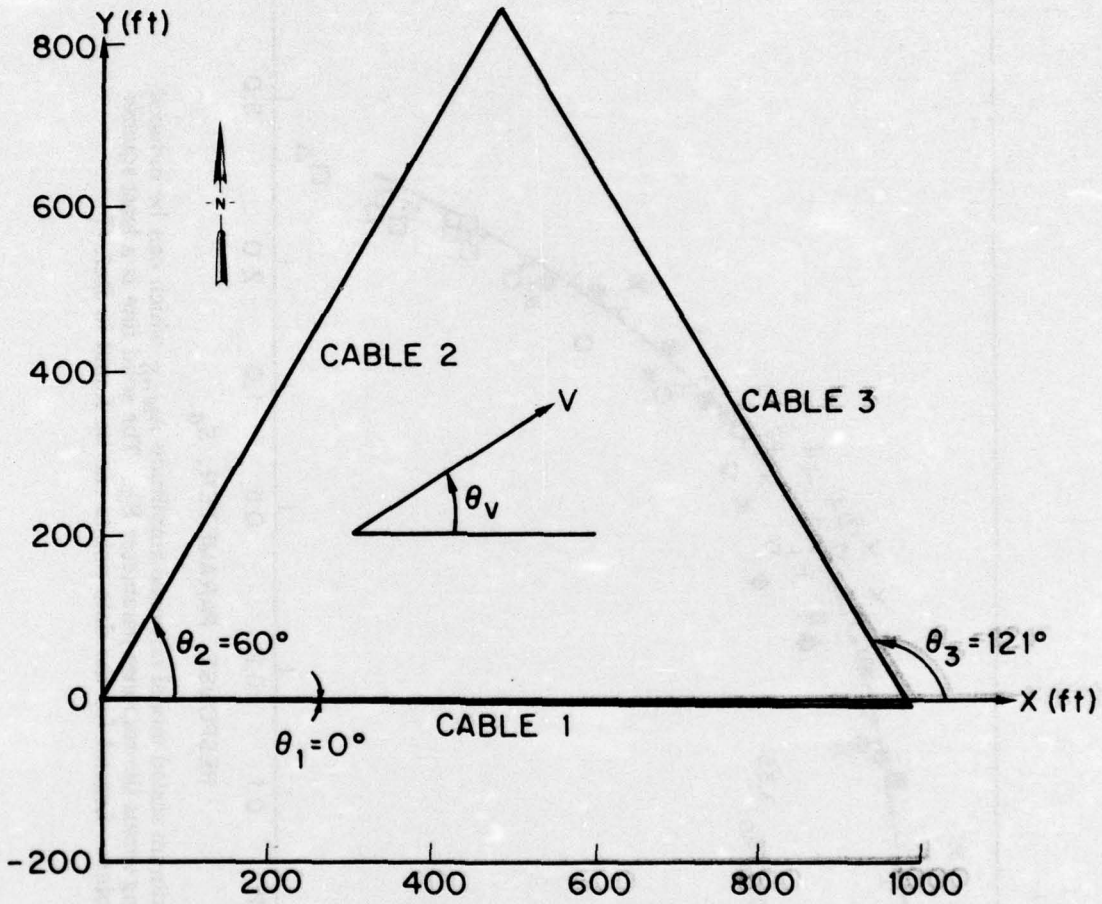

Fig. 5 — Relative orientation of the Seacon II delta referred to an x-y base system. The current at the delta is given by V and the angle of the current with respect to the base system by θ_v.

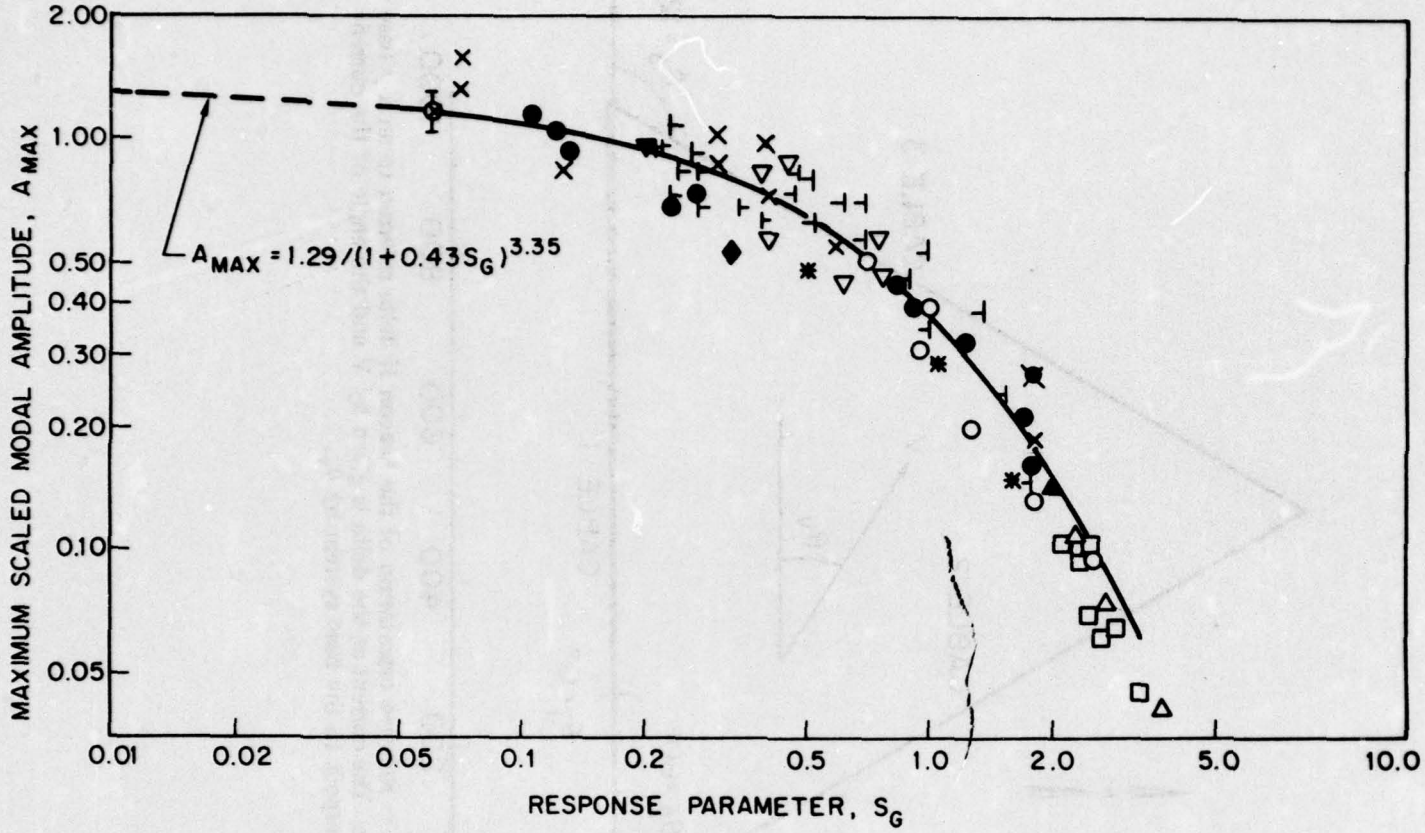

Fig. 6 — The maximum scaled modal response amplitude A_{MAX} which can be induced by vortex shedding versus the response parameter S_G. The solid line is a least squares *fit to the data points. Legend for the data points can be found in* Ref. (7).

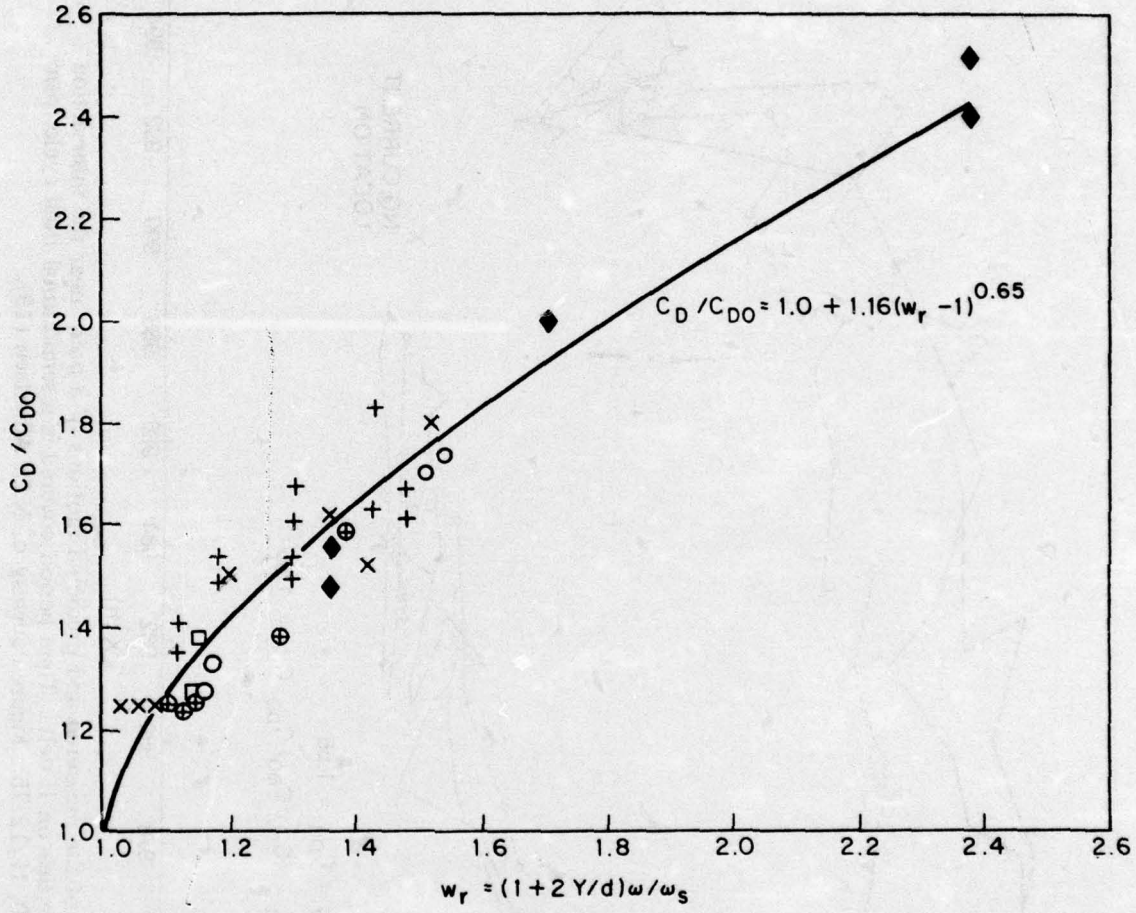

Fig. 7 — The ratio of the drag coefficient C_D on a strumming rigid circular cylinder to the drag coefficient C_{DO} on the stationary cylinder as a function of the wake response parameter w_r. The solid line is a least squares fit to the data points. Legend for the data points: ○ Griffin, Skop, and Koopmann (5); + Griffin and Ramberg (13); □ Ramberg and Griffin (14); ⊕ Tanida, Okajima, and Watanabe (15); X Diana and Falco (16); ◆ Meyers (17).

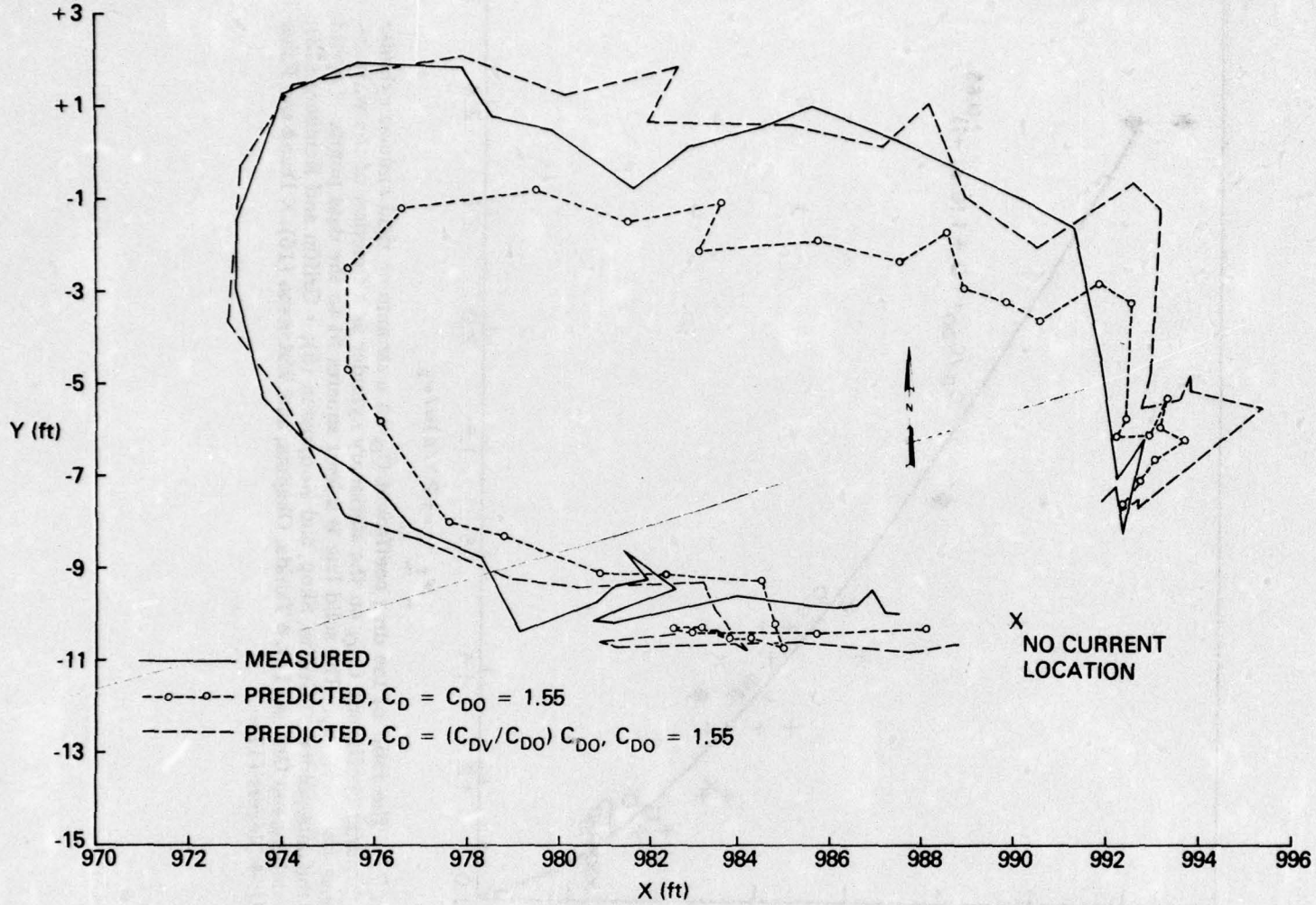

Fig. 8 — A comparison of the measured and predicted motions of a point near the intersection of cables 1 and 3 on the Seacon II delta. Time period covered is a semidiurnal tidal cycle from 2120, 12/11/75 to 0920, 12/12/75. Figure courtesy of N.D. Albertsen (19).